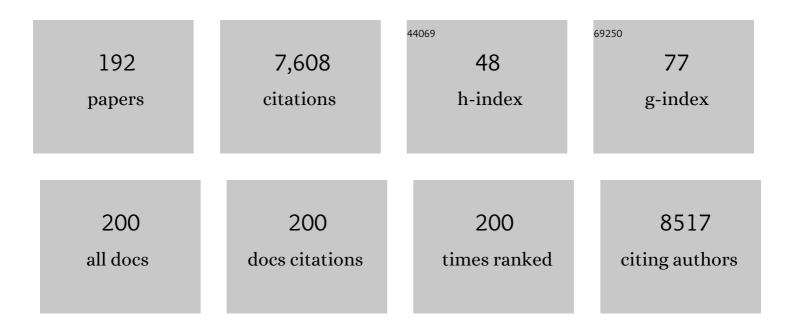
## List of Publications by Year in descending order

Source: https://exaly.com/author-pdf/425667/publications.pdf Version: 2024-02-01



CHIMILI

#	Article	IF	CITATIONS
1	Diversified Regularization Enhanced Training for Effective Manipulator Calibration. IEEE Transactions on Neural Networks and Learning Systems, 2023, 34, 8778-8790.	11.3	39
2	An Lâ,•Norm Based Optimization Method for Sparse Redundancy Resolution of Robotic Manipulators. IEEE Transactions on Circuits and Systems II: Express Briefs, 2022, 69, 469-473.	3.0	10
3	Motion Planning of Manipulators for Simultaneous Obstacle Avoidance and Target Tracking: An RNN Approach With Guaranteed Performance. IEEE Transactions on Industrial Electronics, 2022, 69, 3887-3897.	7.9	30
4	An explicit self-attention-based multimodality CNN in-loop filter for versatile video coding. Multimedia Tools and Applications, 2022, 81, 42497-42511.	3.9	6
5	Approaches to investigate crop responses to ozone pollution: from O <sub>3</sub> â€FACE to satelliteâ€enabled modeling. Plant Journal, 2022, 109, 432-446.	5.7	32
6	Ocean Temperature Prediction Based on Stereo Spatial and Temporal 4-D Convolution Model. IEEE Geoscience and Remote Sensing Letters, 2022, 19, 1-5.	3.1	11
7	An Acceleration-Level Data-Driven Repetitive Motion Planning Scheme for Kinematic Control of Robots With Unknown Structure. IEEE Transactions on Systems, Man, and Cybernetics: Systems, 2022, 52, 5679-5691.	9.3	23
8	Coarse-to-Fine Spatio-Temporal Information Fusion for Compressed Video Quality Enhancement. IEEE Signal Processing Letters, 2022, 29, 543-547.	3.6	5
9	Testing unified theories for ozone response in C <sub>4</sub> species. Global Change Biology, 2022, 28, 3379-3393.	9.5	12
10	Mungbean VrCOL1 regulates flowering time under short-day conditions in Arabidopsis. Plant Cell, Tissue and Organ Culture, 2022, 148, 599-608.	2.3	2
11	A Global Appearance and Local Coding Distortion Based Fusion Framework for CNN Based Filtering in Video Coding. IEEE Transactions on Broadcasting, 2022, 68, 370-382.	3.2	5
12	A Deep Attention Model for Action Recognition from Skeleton Data. Applied Sciences (Switzerland), 2022, 12, 2006.	2.5	6
13	A Modified Fu (1981) Equation with a Time-varying Parameter that Improves Estimates of Inter-annual Variability in Catchment Water Balance. Water Resources Management, 2022, 36, 1645-1659.	3.9	9
14	Effect of Shielding Gas on the Microstructure and Properties of Laser-MAG Hybrid Welded Joint for Nickel-Saving Stainless Steel. Advances in Materials Science and Engineering, 2022, 2022, 1-8.	1.8	2
15	Variable Rate Independently Recurrent Neural Network (IndRNN) for Action Recognition. Applied Sciences (Switzerland), 2022, 12, 3281.	2.5	1
16	Dsa-PAML: a parallel automated machine learning system via dual-stacked autoencoder. Neural Computing and Applications, 2022, 34, 12985-13006.	5.6	1
17	3D printed hydrogel for articular cartilage regeneration. Composites Part B: Engineering, 2022, 237, 109863.	12.0	44
18	3D bioprinting of osteon-mimetic scaffolds with hierarchical microchannels for vascularized bone tissue regeneration. Biofabrication, 2022, 14, 035008.	7.1	18

#	Article	IF	CITATIONS
19	Bioenergy sorghum maintains photosynthetic capacity in elevated ozone concentrations. Plant, Cell and Environment, 2021, 44, 729-746.	5.7	12
20	VrLELP controls flowering time under short-day conditions in Arabidopsis. Journal of Plant Research, 2021, 134, 141-149.	2.4	6
21	Unidirectional movement of small RNAs from shoots to roots in interspecific heterografts. Nature Plants, 2021, 7, 50-59.	9.3	47
22	Functional characterization of soybean (Glycine max) DIRIGENT genes reveals an important role of GmDIR27 in the regulation of pod dehiscence. Genomics, 2021, 113, 979-990.	2.9	12
23	GAS7 Deficiency Promotes Metastasis in MYCN-Driven Neuroblastoma. Cancer Research, 2021, 81, 2995-3007.	0.9	15
24	Characterization of Mungbean CONSTANS-LIKE Genes and Functional Analysis of CONSTANS-LIKE 2 in the Regulation of Flowering Time in Arabidopsis. Frontiers in Plant Science, 2021, 12, 608603.	3.6	13
25	An Anti-Tumor Vaccine Against Marek's Disease Virus Induces Differential Activation and Memory Response of γδT Cells and CD8 T Cells in Chickens. Frontiers in Immunology, 2021, 12, 645426.	4.8	17
26	Formation of Excellent Cathode/Electrolyte Interface with UV-Cured Polymer Electrolyte through In Situ Strategy. Journal of the Electrochemical Society, 2021, 168, 020511.	2.9	10
27	Functionalized gel polymer electrolyte membrane for high performance Li metal batteries. Solid State Ionics, 2021, 361, 115572.	2.7	10
28	Zebrafish as a Neuroblastoma Model: Progress Made, Promise for the Future. Cells, 2021, 10, 580.	4.1	7
29	Mechanochemical synthesis of Li <sub>2</sub> OHI with enhanced lithium ionic conductivity. Functional Materials Letters, 2021, 14, 2150012.	1.2	0
30	Fabrication of Thermoresponsive Hydrogel Scaffolds with Engineered Microscale Vasculatures. Advanced Functional Materials, 2021, 31, 2102685.	14.9	26
31	A composite electrolyte with Na3Zr2Si2PO12 microtube for solid-state sodium-metal batteries. Ceramics International, 2021, 47, 11156-11168.	4.8	13
32	Chimeric HP-PRRSV2 containing an ORF2-6 consensus sequence induces antibodies with broadly neutralizing activity and confers cross protection against virulent NADC30-like isolate. Veterinary Research, 2021, 52, 74.	3.0	15
33	Composite polymer electrolytes with uniform distribution of ionic liquid-grafted ZIF-90 nanofillers for high-performance solid-state Li batteries. Chemical Engineering Journal, 2021, 412, 128733.	12.7	66
34	Au@rGO modified Ni foam as a stable host for lithium metal anode. Solid State Ionics, 2021, 364, 115636.	2.7	5
35	Plant biochemistry influences tropospheric ozone formation, destruction, deposition, and response. Trends in Biochemical Sciences, 2021, 46, 992-1002.	7.5	27
36	Enhanced eletrochemical performances of LiCoO2 at high cut-off voltage by introducing LiF additive. Solid State Ionics, 2021, 365, 115654.	2.7	16

#	Article	IF	CITATIONS
37	A fault diagnosis method based on attention mechanism with application in Qianlong-2 autonomous underwater vehicle. Ocean Engineering, 2021, 233, 109049.	4.3	18
38	Dynamic Non-Gaussian hybrid serial modeling for industrial process monitoring. Chemometrics and Intelligent Laboratory Systems, 2021, 216, 104371.	3.5	7
39	A Novel Ultra-Low Power 8T SRAM-Based Compute-in-Memory Design for Binary Neural Networks. Electronics (Switzerland), 2021, 10, 2181.	3.1	3
40	Gain-of-function of the 1-aminocyclopropane-1-carboxylate synthase gene <i>ACS1G</i> induces female flower development in cucumber gynoecy. Plant Cell, 2021, 33, 306-321.	6.6	31
41	Stable, Low Power and Bit-Interleaving Aware SRAM Memory for Multi-Core Processing Elements. Electronics (Switzerland), 2021, 10, 2724.	3.1	2
42	Inter-Block Dependency-Based CTU Level Rate Control for HEVC. IEEE Transactions on Broadcasting, 2020, 66, 113-126.	3.2	36
43	Antiperovskites with Exceptional Functionalities. Advanced Materials, 2020, 32, e1905007.	21.0	93
44	Characterization and Comparative Analysis of RWP-RK Proteins from <i>Arachis duranensis</i> , <i>Arachis ipaensis</i> , and <i>Arachis hypogaea</i> . International Journal of Genomics, 2020, 2020, 1-19.	1.6	3
45	Mechanism of enhanced ionic conductivity by rotational nitrite group in antiperovskite Na <sub>3</sub> ONO <sub>2</sub> . Journal of Materials Chemistry A, 2020, 8, 21265-21272.	10.3	29
46	Local Structural Changes and Inductive Effects on Ion Conduction in Antiperovskite Solid Electrolytes. Chemistry of Materials, 2020, 32, 8827-8835.	6.7	19
47	Dual redox-active copper hexacyanoferrate nanosheets as cathode materials for advanced sodium-ion batteries. Energy Storage Materials, 2020, 33, 432-441.	18.0	43
48	Ultrathin, dense, hybrid polymer/ceramic gel electrolyte for high energy lithium metal batteries. Materials Letters, 2020, 279, 128480.	2.6	4
49	Genome-wide identification and characterization of nonspecific lipid transfer protein (nsLTP) genes in Arachis duranensis. Genomics, 2020, 112, 4332-4341.	2.9	12
50	Ultrathin, Compacted Gel Polymer Electrolytes Enable Highâ€Energy and Stableâ€Cycling 4 V Lithiumâ€Metal Batteries. ChemElectroChem, 2020, 7, 3656-3662.	3.4	5
51	Complete genome sequence of citrus yellow spot virus, a newly discovered member of the family Betaflexiviridae. Archives of Virology, 2020, 165, 2709-2713.	2.1	2
52	Understanding the electrochemical properties and phase transformations of layered VOPO4â‹H2O as a potassium-ion battery cathode. Journal of Power Sources, 2020, 480, 228864.	7.8	9
53	A Framework of Combining Short-Term Spatial/Frequency Feature Extraction and Long-Term IndRNN for Activity Recognition. Sensors, 2020, 20, 6984.	3.8	9
54	Research Status of Evolution of Microstructure and Properties of Sn-Based Lead-Free Composite Solder Alloys. Journal of Nanomaterials, 2020, 2020, 1-25.	2.7	17

#	Article	IF	CITATIONS
55	Establishing a Multicolor Flow Cytometry to Characterize Cellular Immune Response in Chickens Following H7N9 Avian Influenza Virus Infection. Viruses, 2020, 12, 1396.	3.3	17
56	Corrosion behavior of Sn-based lead-free solder alloys: a review. Journal of Materials Science: Materials in Electronics, 2020, 31, 9076-9090.	2.2	60
57	Role of the calcite-water interface in wettability alteration during low salinity waterflooding. Fuel, 2020, 276, 118097.	6.4	15
58	A Novel FPGA Accelerator Design for Real-Time and Ultra-Low Power Deep Convolutional Neural Networks Compared With Titan X GPU. IEEE Access, 2020, 8, 105455-105471.	4.2	34
59	Europium-Doped Ceria Nanowires as Anode for Solid Oxide Fuel Cells. Frontiers in Chemistry, 2020, 8, 348.	3.6	11
60	Novel CNN-Based AP2D-Net Accelerator: An Area and Power Efficient Solution for Real-Time Applications on Mobile FPGA. Electronics (Switzerland), 2020, 9, 832.	3.1	9
61	Al on a chip. Lab on A Chip, 2020, 20, 3074-3090.	6.0	80
62	The R-Loop Atlas of Arabidopsis Development and Responses to Environmental Stimuli. Plant Cell, 2020, 32, 888-903.	6.6	61
63	Rapid Fabrication of Ready-to-Use Gelatin Scaffolds with Prevascular Networks Using Alginate Hollow Fibers as Sacrificial Templates. ACS Biomaterials Science and Engineering, 2020, 6, 2297-2311.	5.2	17
64	B-box Proteins in Arachis duranensis: Genome-Wide Characterization and Expression Profiles Analysis. Agronomy, 2020, 10, 23.	3.0	18
65	Zeta potential in intact carbonates at reservoir conditions and its impact on oil recovery during controlled salinity waterflooding. Fuel, 2020, 266, 116927.	6.4	46
66	Self-Regulated Phenomenon of Inorganic Artificial Solid Electrolyte Interphase for Lithium Metal Batteries. Nano Letters, 2020, 20, 4029-4037.	9.1	78
67	Occurrence and molecular characterization of apple scarÂskin viroid in Malus pumila â€~Saiwaihong' (small apple tree) from North China. Journal of Plant Pathology, 2020, 102, 899-902.	1.2	2
68	Dendrobium viroid, a new monocot-infecting apscaviroid. Virus Research, 2020, 282, 197958.	2.2	8
69	Low-Power RTL Code Generation for Advanced CNN Algorithms toward Object Detection in Autonomous Vehicles. Electronics (Switzerland), 2020, 9, 478.	3.1	12
70	Automated Detection of Commissioning Changes in Connected Lighting Systems. IEEE Internet of Things Journal, 2019, 6, 898-905.	8.7	10
71	Recurrent Neural Network for Kinematic Control of Redundant Manipulators With Periodic Input Disturbance and Physical Constraints. IEEE Transactions on Cybernetics, 2019, 49, 4194-4205.	9.5	77
72	Plume Front Tracking in Unknown Environments by Estimation and Control. IEEE Transactions on Industrial Informatics, 2019, 15, 911-921.	11.3	24

#	Article	IF	CITATIONS
73	Variations in Rating Scale Functioning in Assessing Speech Act Production in L2 Chinese. Language Assessment Quarterly, 2019, 16, 271-293.	2.0	12
74	Influence of cyclic non-isothermal heat treatment on microstructure, mechanical property and corrosion behavior of Al–Zn–Mg alloy. Materials Research Express, 2019, 6, 096501.	1.6	4
75	Nanobundles of Iron Phosphide Fabricated by Direct Phosphorization of Metal–Organic Frameworks as an Efficient Hydrogenâ€Evolving Electrocatalyst. Chemistry - A European Journal, 2019, 26, 4001.	3.3	13
76	Molecular and transcriptional characterization of phosphatidyl ethanolamine-binding proteins in wild peanuts Arachis duranensis and Arachis ipaensis. BMC Plant Biology, 2019, 19, 484.	3.6	17
77	The Effects of Heat Straightening Temperature on the Microstructure and Properties of 7N01 Aluminum Alloy. Materials, 2019, 12, 2949.	2.9	12
78	Identification of Two Porcine Reproductive and Respiratory Syndrome Virus Variants Sharing High Genomic Homology but with Distinct Virulence. Viruses, 2019, 11, 875.	3.3	22
79	Development of universal and quadruplex realâ€time RTâ€PCR assays for simultaneous detection and differentiation of porcine reproductive and respiratory syndrome viruses. Transboundary and Emerging Diseases, 2019, 66, 2271-2278.	3.0	36
80	Quenching Sensitivity of Al-Zn-Mg Alloy after Non-Isothermal Heat Treatment. Materials, 2019, 12, 1595.	2.9	9
81	Deletion of kallikrein 1b5 ( <i>Klk1b5</i> ) has no impact on fertility in mice. Molecular Reproduction and Development, 2019, 86, 611-613.	2.0	0
82	Classification of Occupancy Sensor Anomalies in Connected Indoor Lighting Systems. IEEE Internet of Things Journal, 2019, 6, 7175-7182.	8.7	11
83	Elevated Ozone Concentration Reduces Photosynthetic Carbon Gain but Does Not Alter Leaf Structural Traits, Nutrient Composition or Biomass in Switchgrass. Plants, 2019, 8, 85.	3.5	15
84	Genetic Regulation of Ethylene Dosage for Cucumber Fruit Elongation. Plant Cell, 2019, 31, 1063-1076.	6.6	85
85	Exploiting Pulping Waste as an Ecofriendly Multifunctional Binder for Lithium Sulfur Batteries. ACS Sustainable Chemistry and Engineering, 2019, 7, 8413-8418.	6.7	21
86	Molecular Characterization and Expression Profile Analysis of Heat Shock Transcription Factors in Mungbean. Frontiers in Genetics, 2019, 9, 736.	2.3	16
87	Ca-doped Na2Zn2TeO6 layered sodium conductor for all-solid-state sodium-ion batteries. Electrochimica Acta, 2019, 298, 121-126.	5.2	40
88	Co-infection status of classical swine fever virus (CSFV), porcine reproductive and respiratory syndrome virus (PRRSV) and porcine circoviruses (PCV2 and PCV3) in eight regions of China from 2016 to 2018. Infection, Genetics and Evolution, 2019, 68, 127-135.	2.3	62
89	Ultrafast Sodium/Potassiumâ€ion Intercalation into Hierarchically Porous Thin Carbon Shells. Advanced Materials, 2019, 31, e1805430.	21.0	214
00	A novel <scp>NADC</scp> 30â€like porcine reproductive and respiratory syndrome virus () Tj ETQq0 0 0 rgBT		
90		3.0	23

#	Article	IF	CITATIONS
91	Influence of Conductive additives on the stability of red phosphorus-carbon anodes for sodium-ion batteries. Scientific Reports, 2019, 9, 946.	3.3	12
92	Neural Dynamics for Cooperative Control of Redundant Robot Manipulators. IEEE Transactions on Industrial Informatics, 2018, 14, 3812-3821.	11.3	151
93	Multimode processes monitoring based on hierarchical mode division and subspace decomposition. Canadian Journal of Chemical Engineering, 2018, 96, 2420-2430.	1.7	12
94	Thermally Stable and Tough Coatings and Films Using Vinyl Silylated Lignin. ACS Sustainable Chemistry and Engineering, 2018, 6, 1988-1998.	6.7	22
95	Elevation of soybean seed oil content through selection for seed coat shininess. Nature Plants, 2018, 4, 30-35.	9.3	75
96	Glandular trichomes as a barrier against atmospheric oxidative stress: Relationships with ozone uptake, leaf damage, and emission of LOX products across a diverse set of species. Plant, Cell and Environment, 2018, 41, 1263-1277.	5.7	69
97	Ozone-triggered surface uptake and stress volatile emissions in Nicotiana tabacum â€~Wisconsin'. Journal of Experimental Botany, 2018, 69, 681-697.	4.8	26
98	Multimode Processes Monitoring Using Global–Local MIC-PCA-SVDD. Lecture Notes in Electrical Engineering, 2018, , 307-320.	0.4	1
99	A Fusion Framework for Camouflaged Moving Foreground Detection in the Wavelet Domain. IEEE Transactions on Image Processing, 2018, 27, 3918-3930.	9.8	32
100	Hole Filling With Multiple Reference Views in DIBR View Synthesis. IEEE Transactions on Multimedia, 2018, 20, 1948-1959.	7.2	60
101	Modified Primal-Dual Neural Networks for Motion Control of Redundant Manipulators With Dynamic Rejection of Harmonic Noises. IEEE Transactions on Neural Networks and Learning Systems, 2018, 29, 4791-4801.	11.3	115
102	Strawberry vein banding virus P6 protein intracellular transport and an important domain identification. Journal of Integrative Agriculture, 2018, 17, 2031-2041.	3.5	2
103	Strawberry Vein Banding Virus P6 Protein Is a Translation Trans-Activator and Its Activity Can be Suppressed by FveIF3g. Viruses, 2018, 10, 717.	3.3	9
104	Anomalous Zeta Potential Trends in Natural Sandstones. Geophysical Research Letters, 2018, 45, 11,068.	4.0	12
105	Glycinamide modified polyacrylic acid as high-performance binder for silicon anodes in lithium-ion batteries. Journal of Power Sources, 2018, 406, 102-109.	7.8	66
106	Novel Lignin-Derived Water-Soluble Binder for Micro Silicon Anode in Lithium-Ion Batteries. ACS Sustainable Chemistry and Engineering, 2018, 6, 12621-12629.	6.7	68
107	Atomic layered deposition iron oxide on perovskite LaNiO3 as an efficient and robust bi-functional catalyst for lithium oxygen batteries. Electrochimica Acta, 2018, 281, 338-347.	5.2	57
108	Identification of Strawberry vein banding virus encoded P6 as an RNA silencing suppressor. Virology, 2018, 520, 103-110.	2.4	18

#	Article	IF	CITATIONS
109	Fallopian Tube/Oviduct: Structure and Cell Biology. , 2018, , 282-290.		1
110	Embryo Transport. , 2018, , 357-363.		1
111	Estrogen Action in the Epithelial Cells of the Mouse Vagina Regulates Neutrophil Infiltration and Vaginal Tissue Integrity. Scientific Reports, 2018, 8, 11247.	3.3	46
112	Emergence of a novel highly pathogenic recombinant virus from three lineages of porcine reproductive and respiratory syndrome virus 2 in China 2017. Transboundary and Emerging Diseases, 2018, 65, 1775-1785.	3.0	46
113	Neural Network-Based Model-Free Adaptive Near-Optimal Tracking Control for a Class of Nonlinear Systems. IEEE Transactions on Neural Networks and Learning Systems, 2018, 29, 6227-6241.	11.3	35
114	Developing a test of L2 Chinese pragmatic comprehension ability. Language Testing in Asia, 2018, 8, .	1.9	6
115	Pitch imperfect. Science, 2018, 360, 678-678.	12.6	0
116	Parallel domestication with a broad mutational spectrum of determinate stem growth habit in leguminous crops. Plant Journal, 2018, 96, 761-771.	5.7	27
117	Risk Detection of Stroke Using a Feature Selection and Classification Method. IEEE Access, 2018, 6, 31899-31907.	4.2	20
118	Estrogen receptor $\hat{I}_{\pm}$ is required for oviductal transport of embryos. FASEB Journal, 2017, 31, 1595-1607.	0.5	50
119	Manipulability Optimization of Redundant Manipulators Using Dynamic Neural Networks. IEEE Transactions on Industrial Electronics, 2017, 64, 4710-4720.	7.9	286
120	Predictive Suboptimal Consensus of Multiagent Systems With Nonlinear Dynamics. IEEE Transactions on Systems, Man, and Cybernetics: Systems, 2017, 47, 1701-1711.	9.3	56
121	Distributed Biased Min-Consensus With Applications to Shortest Path Planning. IEEE Transactions on Automatic Control, 2017, 62, 5429-5436.	5.7	75
122	A type of biased consensus-based distributed neural network for path planning. Nonlinear Dynamics, 2017, 89, 1803-1815.	5.2	33
123	A Robust Algorithm for State-of-Charge Estimation With Gain Optimization. IEEE Transactions on Industrial Informatics, 2017, 13, 2983-2994.	11.3	39
124	Two h-Type Thioredoxins Interact with the E2 Ubiquitin Conjugase PHO2 to Fine-Tune Phosphate Homeostasis in Rice. Plant Physiology, 2017, 173, 812-824.	4.8	46
125	Ozoneâ€induced foliar damage and release of stress volatiles is highly dependent on stomatal openness and priming by lowâ€level ozone exposure in <scp><i>Phaseolus vulgaris</i></scp> . Plant, Cell and Environment, 2017, 40, 1984-2003.	5.7	66
126	Simultaneous learning and control of parallel Stewart platforms with unknown parameters. Neurocomputing, 2017, 266, 114-122.	5.9	33

#	Article	IF	CITATIONS
127	Nonconvex function activated zeroing neural network models for dynamic quadratic programming subject to equality and inequality constraints. Neurocomputing, 2017, 267, 107-113.	5.9	78
128	Nanocellulose and Its Derivatives for High-Performance Water-Based Fluids. , 2017, , .		17
129	Molecular interaction between PHO2 and GIGANTEA reveals a new crosstalk between flowering time and phosphate homeostasis in <scp><i>Oryza sativa</i></scp> . Plant, Cell and Environment, 2017, 40, 1487-1499.	5.7	49
130	Plasticity and innovation of regulatory mechanisms underlying seed oil content mediated by duplicated genes in the palaeopolyploid soybean. Plant Journal, 2017, 90, 1120-1133.	5.7	51
131	Two novel porcine epidemic diarrhea virus (PEDV) recombinants from a natural recombinant and distinct subtypes of PEDV variants. Virus Research, 2017, 242, 90-95.	2.2	46
132	Characterization of Engineered Scaffolds with Spatial Prevascularized Networks for Bulk Tissue Regeneration. ACS Biomaterials Science and Engineering, 2017, 3, 2493-2501.	5.2	9
133	Correlated and weakly correlated fault detection based on variable division and ICA. Computers and Industrial Engineering, 2017, 112, 320-335.	6.3	40
134	Zeroing neural networks: A survey. Neurocomputing, 2017, 267, 597-604.	5.9	150
135	Oviduct: roles in fertilization and early embryo development. Journal of Endocrinology, 2017, 232, R1-R26.	2.6	175
136	Kinematic Control of Redundant Manipulators Using Neural Networks. IEEE Transactions on Neural Networks and Learning Systems, 2017, 28, 2243-2254.	11.3	238
137	Methyl jasmonate-induced emission of biogenic volatiles is biphasic in cucumber: a high-resolution analysis of dose dependence. Journal of Experimental Botany, 2017, 68, 4679-4694.	4.8	60
138	Collection of Post-mating Semen from the Female Reproductive Tract and Measurement of Semen Liquefaction in Mice. Journal of Visualized Experiments, 2017, , .	0.3	3
139	Symmetric and Nonnegative Latent Factor Models for Undirected, High-Dimensional, and Sparse Networks in Industrial Applications. IEEE Transactions on Industrial Informatics, 2017, 13, 3098-3107.	11.3	128
140	Conditional knockout mice for the distal appendage protein CEP164 reveal its essential roles in airway multiciliated cell differentiation. PLoS Genetics, 2017, 13, e1007128.	3.5	57
141	Plk1 is essential for proper chromosome segregation during meiosis I/meiosis II transition in pig oocytes. Reproductive Biology and Endocrinology, 2017, 15, 69.	3.3	9
142	Crucial role of estrogen for the mammalian female in regulating semen coagulation and liquefaction in vivo. PLoS Genetics, 2017, 13, e1006743.	3.5	15
143	Morphological Diversity of the Rod Spherule: A Study of Serially Reconstructed Electron Micrographs. PLoS ONE, 2016, 11, e0150024.	2.5	15
144	Mutation of OsGIGANTEA Leads to Enhanced Tolerance to Polyethylene Glycol-Generated Osmotic Stress in Rice. Frontiers in Plant Science, 2016, 7, 465.	3.6	17

#	Article	IF	CITATIONS
145	Enhanced ionic conductivity with Li7O2Br3 phase in Li3OBr anti-perovskite solid electrolyte. Applied Physics Letters, 2016, 109, .	3.3	48
146	A novel method for fabricating engineered structures with branched micro-channel using hollow hydrogel fibers. Biomicrofluidics, 2016, 10, 064104.	2.4	15
147	A Versatile Method for Fabricating Tissue Engineering Scaffolds with a Three-Dimensional Channel for Prevasculature Networks. ACS Applied Materials & amp; Interfaces, 2016, 8, 25096-25103.	8.0	50
148	Fine mapping and candidate gene analysis of two loci conferring resistance to Phytophthora sojae in soybean. Theoretical and Applied Genetics, 2016, 129, 2379-2386.	3.6	54
149	Carboxymethylated lignins with low surface tension toward low viscosity and highly stable emulsions of crude bitumen and refined oils. Journal of Colloid and Interface Science, 2016, 482, 27-38.	9.4	31
150	Oilâ€inâ€Water Emulsions Stabilized by Carboxymethylated Lignins: Properties and Energy Prospects. ChemSusChem, 2016, 9, 2460-2469.	6.8	46
151	Mono- and sesquiterpene release from tomato ( Solanum lycopersicum ) leaves upon mild and severe heat stress and through recovery: From gene expression to emission responses. Environmental and Experimental Botany, 2016, 132, 1-15.	4.2	51
152	Antioxidant and Thermal Stabilization of Polypropylene by Addition of Butylated Lignin at Low Loadings. ACS Sustainable Chemistry and Engineering, 2016, 4, 5248-5257.	6.7	52
153	Modified ZNN for Time-Varying Quadratic Programming With Inherent Tolerance to Noises and Its Application to Kinematic Redundancy Resolution of Robot Manipulators. IEEE Transactions on Industrial Electronics, 2016, 63, 6978-6988.	7.9	194
154	Interfacial Stabilization of Fiber-Laden Foams with Carboxymethylated Lignin toward Strong Nonwoven Networks. ACS Applied Materials & Interfaces, 2016, 8, 19827-19835.	8.0	21
155	Fluorineâ€Doped Antiperovskite Electrolyte for Allâ€Solidâ€State Lithiumâ€Ion Batteries. Angewandte Chemie - International Edition, 2016, 55, 9965-9968.	13.8	192
156	Sodium Ion Transport Mechanisms in Antiperovskite Electrolytes Na <sub>3</sub> OBr and Na <sub>4</sub> OI <sub>2</sub> : An <i>in Situ</i> Neutron Diffraction Study. Inorganic Chemistry, 2016, 55, 5993-5998.	4.0	68
157	IPLaminator: an ImageJ plugin for automated binning and quantification of retinal lamination. BMC Bioinformatics, 2016, 17, 36.	2.6	8
158	Regulation of Floral Terpenoid Emission and Biosynthesis in Sweet Basil (Ocimum basilicum). Journal of Plant Growth Regulation, 2016, 35, 921-935.	5.1	16
159	Antiperovskite Li <sub>3</sub> OCl Superionic Conductor Films for Solidâ€&tate Liâ€Ion Batteries. Advanced Science, 2016, 3, 1500359.	11.2	162
160	Influence of surface conductivity on the apparent zeta potential of calcite. Journal of Colloid and Interface Science, 2016, 468, 262-275.	9.4	80
161	Reaction mechanism studies towards effective fabrication of lithium-rich anti-perovskites Li3OX (X=) Tj ETQq1 1	0.784314 2.7	rgBT /Over
162	Inverse-Free Extreme Learning Machine With Optimal Information Updating. IEEE Transactions on	9.5	111

Cybernetics, 2016, 46, 1229-1241.

#	Article	IF	CITATIONS
163	Innovation of a Regulatory Mechanism Modulating Semi-determinate Stem Growth through Artificial Selection in Soybean. PLoS Genetics, 2016, 12, e1005818.	3.5	48
164	Performance, combustion, and emissions in a diesel engine operated with fuel-in-water emulsions based on lignin. Applied Energy, 2015, 154, 851-861.	10.1	120
165	Structural manipulation approaches towards enhanced sodium ionic conductivity in Na-rich antiperovskites. Journal of Power Sources, 2015, 293, 735-740.	7.8	97
166	Monitoring of Multimode Processes Based on Subspace Decomposition. Industrial & Engineering Chemistry Research, 2015, 54, 3855-3864.	3.7	18
167	DSCAM Promotes Refinement in the Mouse Retina through Cell Death and Restriction of Exploring Dendrites. Journal of Neuroscience, 2015, 35, 5640-5654.	3.6	43
168	Mutation in xyloglucan 6-xylosytransferase results in abnormal root hair development in Oryza sativa. Journal of Experimental Botany, 2014, 65, 4149-4157.	4.8	52
169	Cooperative Distributed Source Seeking by Multiple Robots: Algorithms and Experiments. IEEE/ASME Transactions on Mechatronics, 2014, 19, 1810-1820.	5.8	132
170	Modeling and monitoring of nonlinear multi-mode processes. Control Engineering Practice, 2014, 22, 194-204.	5.5	46
171	Oxygen deficit alleviates phosphate overaccumulation toxicity in OsPHR2 overexpression plants. Journal of Plant Research, 2014, 127, 433-440.	2.4	9
172	Heterogeneity of anatomical structure in giant leaves of <italic>Musa balbisiana</italic> . Chinese Science Bulletin, 2014, 59, 522-528.	0.7	2
173	Modeling and Monitoring Between-Mode Transition of Multimodes Processes. IEEE Transactions on Industrial Informatics, 2013, 9, 2248-2255.	11.3	51
174	Perovskite Sr <sub>1–<i>x</i></sub> Ce <sub><i>x</i></sub> CoO <sub>3â^î^</sub> (0.05 ≤i>x ≤0.15 Superior Cathodes for Intermediate Temperature Solid Oxide Fuel Cells. ACS Applied Materials & Interfaces, 2013, 5, 1143-1148.	5) as 8.0	87
175	Mycobacterium bovis and BCG induce different patterns of cytokine and chemokine production in dendritic cells and differentiation patterns in CD4+ T cells. Microbiology (United Kingdom), 2013, 159, 366-379.	1.8	20
176	The Heterogeneity and Spatial Patterning of Structure and Physiology across the Leaf Surface in Giant Leaves of Alocasia macrorrhiza. PLoS ONE, 2013, 8, e66016.	2.5	25
177	Dynamical process monitoring using dynamical hierarchical kernel partial least squares. Chemometrics and Intelligent Laboratory Systems, 2012, 118, 150-158.	3.5	26
178	Improved multi-scale kernel principal component analysis and its application for fault detection. Chemical Engineering Research and Design, 2012, 90, 1271-1280.	5.6	56
179	Functional characterization of the rice <i>SPXâ€MFS</i> family reveals a key role of <i>OsSPXâ€MFS1</i> in controlling phosphate homeostasis in leaves. New Phytologist, 2012, 196, 139-148.	7.3	139
180	A Novel Mouse Dscam Mutation Inhibits Localization and Shedding of DSCAM. PLoS ONE, 2012, 7, e52652.	2.5	27

#	Article	IF	CITATIONS
181	Perovskite Sr0.95Ce0.05CoO3â^î′ loaded with copper nanoparticles as a bifunctional catalyst for lithium-air batteries. Journal of Materials Chemistry, 2012, 22, 18902.	6.7	131
182	Dynamic processes monitoring using recursive kernel principal component analysis. Chemical Engineering Science, 2012, 72, 78-86.	3.8	94
183	Feasibility and mechanism of lithium oxide as sintering aid for Ce0.8Sm0.2Oδ electrolyte. Journal of Power Sources, 2012, 205, 57-62.	7.8	40